

Mesenchymal-epithelial transition in development and reprogramming

Duanqing Pei^{1,2*}, Xiaodong Shu^{1,2}, Ama Gassama-Diagne^{3,4} and Jean Paul Thiery^{1,5,6,7,8*}

During organogenesis, epithelial cells can give rise to mesenchymal cells through epithelial-mesenchymal transition. The reverse process, mesenchymal-epithelial transition (MET), can similarly generate epithelial cells. Transitions between epithelial and mesenchymal states are also critical for the induction of pluripotent stem cells from somatic cells. This Review discusses the relatively less characterized process of MET, focusing on the genesis of apicobasal cell polarity and exploring the roles of MET in development and reprogramming.

Epithelial-mesenchymal transition (EMT) and its reverse process mesenchymal-epithelial transition (MET) are fundamental evolutionarily conserved mechanisms employed at different stages of morphogenesis and organogenesis to generate the body plan of metazoans. EMT involves the progressive loss of epithelial cell polarity, downregulation of junctional complexes and reorganization of the actin cytoskeleton to confer the migratory phenotype necessary to execute the extensive cellular movements that will give rise to the germ layers and later to tissues¹. MET is employed to generate epithelia at different developmental stages. During MET, mesenchymal cells progressively establish apicobasal polarity through an evolutionarily conserved group of proteins and distinct but well-defined mechanisms²: polarity-related cell-surface receptors generate different membrane domains and become stabilized with the assembly of junctional complexes, leading to the formation of tight junctions at the apex of the lateral domain and the organization of cytoskeletal structures and organelles². Evidence of embryonic cells displaying attributes of both epithelial and mesenchymal phenotypes supports the existence of transient intermediate EMT and MET stages²⁻⁵, a phenomenon that is also observed in carcinoma^{1,6}.

Long germ-band insects, such as *Drosophila*, assemble the first epithelium through the migration of nuclei to the periphery of the egg followed by rapid cellularization^{7,8}. The newly formed epithelial blastoderm will engage in complex morphogenetic movements to elongate the embryo and simultaneously create invagination sites by the localized formation of a contractile actomyosin ring in cells within the body cavity. This process initiates gastrulation at distinct sites along the body axis⁷. Endodermal cells forming the anterior and posterior proctodaeal invaginations engage in an EMT-MET sequence and merge to give rise to the midgut. By contrast, ectodermal cells that form the foregut and the hindgut will retain their epithelial phenotype^{7,8}. An EMT-MET cycle is also observed for mesodermal cells that invaginate through the ventral furrow to form the dorsal vessel gonadal sheet and the Malpighian tubules⁹. Most other metazoan development proceeds through a series of cleavages of the fertilized egg and the progressive assembly of epithelial-like structures. These embryos engage in gastrulation by activating epithelial plasticity programmes, including EMT, as soon as the blastocoelic cavity is

formed¹⁰. Although morphogenetic movements are quite diverse in different species, they adhere to a set of general principles of epithelial cell plasticity, reviewed in detail elsewhere¹¹.

Embryonic stem cells (ESCs) or induced pluripotent stem cells (iPSCs) undergo EMT and MET to differentiate into somatic cell types. Similarly, differentiated somatic cells can be reprogrammed into pluripotent cells by a sequential EMT-MET, with MET being a critical step for the acquisition of pluripotency¹². In addition to the establishment of epithelial polarity, MET in reprogramming is associated with metabolic switching, epigenetic modifications and cell fate changes¹³, providing a unique opportunity to investigate the relationships between these cellular events.

Although morphogenesis and setting the body plan require cell plasticity and EMT-MET cycles, later postnatal development requires stabilization of epithelial tissues. EMT-associated transcription factors are rarely detectable in adult epithelial tissues¹⁴ and several factors were recently shown to protect this epithelial state. For instance, inactivation of the Ets superfamily transcription factor ELF5 induces EMT in the normal mammary gland, affecting alveologenesis and increasing the number of mammary stem cells¹⁵. In vitro, ELF5 overexpression prevents transforming growth factor- β (TGF- β)-induced EMT in normal murine mammary cells and can partially revert the mesenchymal phenotype of breast adenocarcinoma cells¹⁵. Grainyhead-like 2 (GRHL2), a DNA-binding protein that maintains the non-neural ectodermal epithelium¹⁶, binds to *CDH1* (which encodes E-cadherin) intron 2 and the promoter of *CLDN4* (which encodes claudin-4) to augment their transcription^{17,18}. As a result, *GRHL2* suppression induces a mesenchymal-like phenotype in ovarian epithelial carcinoma cell lines. Finally, the *Ovol1* and *Ovol2* transcription factors maintain epithelial integrity in the embryonic epidermis¹⁹ and *Ovol2* also in the mammary gland²⁰, by repressing EMT-associated transcription factors. One such factor, *Zeb1*, is controlled by a regulatory loop involving repression directly by *GRHL2* and *Ovol2* or indirectly through microRNA-200 (ref. 18).

This Review focuses on the mechanisms that drive the induction and maintenance of epithelial tissues in development, the molecular drivers that contribute to epithelial cell polarization and the role of MET in reprogramming.

¹CAS Key Laboratory of Regenerative Biology, Guangdong Provincial Key Laboratory of Stem Cell and Regenerative Medicine, South China Institute for Stem Cell Biology and Regenerative Medicine, Guangzhou Institutes of Biomedicine and Health, Chinese Academy of Sciences, Guangzhou, China.

²Guangzhou Regenerative Medicine and Health Guangdong Laboratory at GIBH, Guangzhou, China. ³INSERM, Unité, 1193 Villejuif, France. ⁴Université Paris-Sud, UMR-S 1193, Villejuif, France. ⁵Department of Biochemistry, Yong Loo Lin School of Medicine, National University of Singapore, Singapore, Singapore. ⁶CNRS UMR 7057 Matter and Complex Systems, University Paris Denis Diderot, Paris, France. ⁷INSERM Unit 1186, Comprehensive Cancer Center, Institut Gustave Roussy, Villejuif, France. ⁸Drug Discovery Pipeline, Guangzhou Institutes of Biomedicine and Health, Chinese Academy of Science, Guangzhou, China. *e-mail: pei_duanqing@gibh.ac.cn; bchtjp@nus.edu.sg

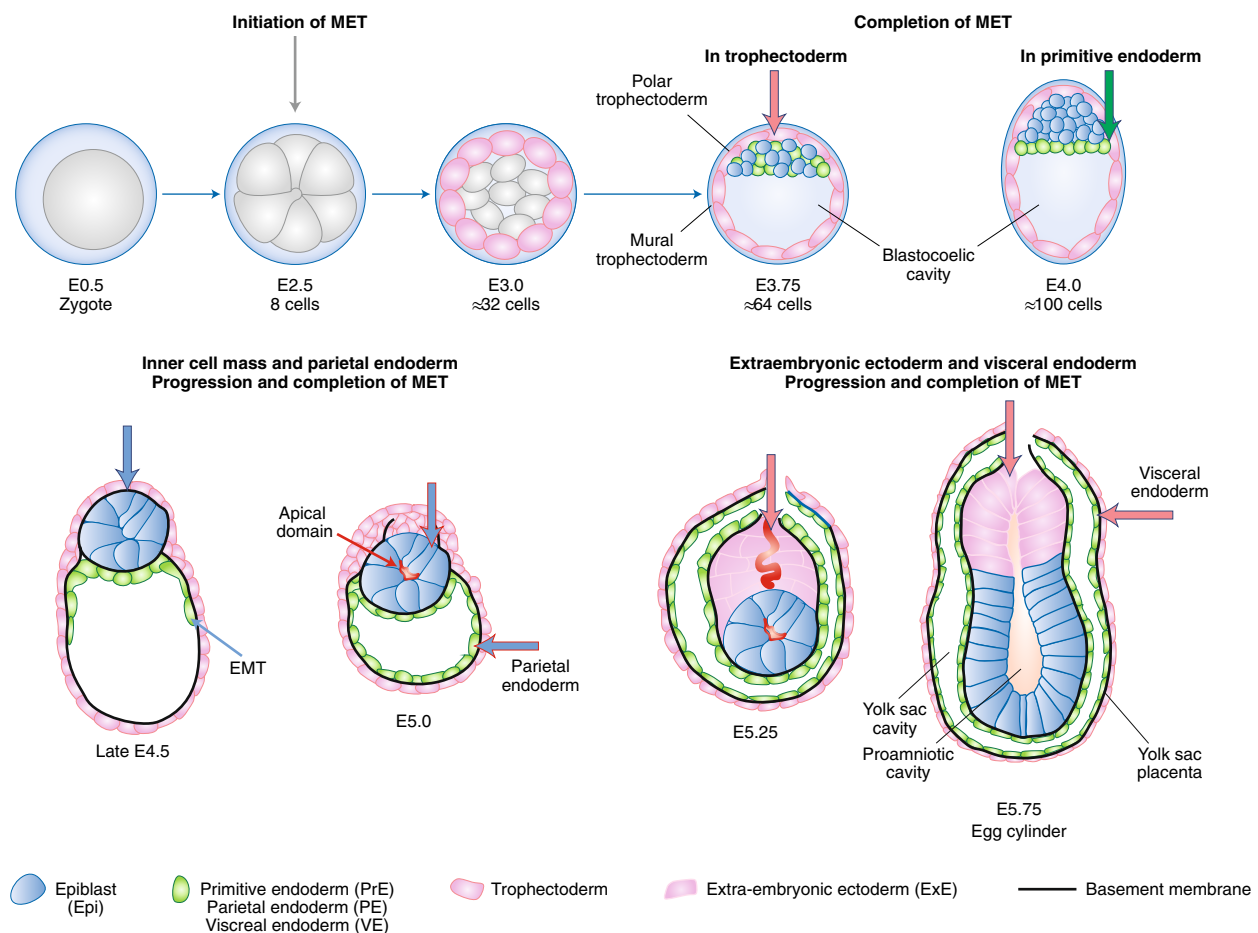


Fig. 1 | Formation of the first epithelia in the mouse embryo through MET. Following fertilization, the mouse egg enters cell division through cleavages. At E2.5, blastomeres maximize their intercellular contacts through compaction as a first step of MET. This mechanism is essential for the formation of the trophectoderm, which segregates as an outer layer at the 32-cell stage, a time at which these cells engage the MET programme. By E3.75, the trophectoderm has acquired a fully polarized epithelial structure, with functional tight junctions permitting the formation of the first cavity (the blastocoelic cavity). By E4.0, MET initiates in the primitive endodermal cells sorting them from the ICM (blue). A basement membrane is produced by the trophectoderm and the primitive endoderm, separating these two extraembryonic tissues from the ICM. By E4.5, the primitive endoderm expands along the mural trophectoderm and undergoes partial EMT at the leading edge (late E4.5). The mural trophectoderm and the parietal endoderm are separated by a basement membrane. By E4.75, cells in the ICM start reorganizing their intercellular contacts to acquire an apicobasal polarity. This polarity is initiated by acquiring a basal domain identity in contact with the newly deposited basement membrane that interacts with β_1 -integrins. Par6 and aPKC accumulate at the apical domain, which is narrowing by a contractile actomyosin ring, a region that is becoming enriched in E-cadherin-based adherens junctions. These events confer a rosette-like structure to the ICM. At E5.0, MET is fully executed, with a small cavity forming at the apical domain by hollowing through the repulsive interactions of apically expressed podocalyxin. At E5.25, a similar reorganization occurs in the extraembryonic ectoderm to generate an apicobasal polarity. The newly formed lumen in the extraembryonic ectoderm will merge with the ectoderm lumen to create the amniotic cavity at the egg cylinder stage. The thicker coloured arrows indicate the time of initiation or completion of MET in the different cell layers.

MET in development

MET is a fundamental process in histogenesis to assemble mesenchymal-like cells into cohesive structures. In the absence of MET, embryos cannot engage in gastrulation or the subsequent body plan formation.

Epithelia in eutherian mammals. Trophectoderm. In mammalian embryos, the need to implant at an early stage after the first round of cleavages prioritizes the formation of the trophectoderm before epithelial characteristics are acquired by the primitive endoderm and the epiblast. MET operates only after the first three cleavages (Fig. 1). The resulting 8-cell mouse embryo undergoes compaction—a well-studied process that is critical for the first lineage segregation at the next cell division. At the 16-cell stage, cells located at the periphery of the morula will be destined to form the epithelial trophectoderm,

which is required for ensuring implantation in the endometrium. These cells exhibit asymmetric cell contacts compared to those cells in the inner cell mass (ICM). The trophectoderm cells become polarized at this stage, and during the next cell division, trophectodermal cells assemble adherens junctions, desmosomes, gap junctions and, most importantly, tight junctions, which permit the selective paracellular transport of ions and water to create the blastocoelic cavity. Transcripts of tight junction proteins, including junctional adhesion molecules and zonula occludens-1 (ZO-1), are already detected at the 8-cell stage, but these proteins are translated and post-translationally modified only at the 16-cell to 32-cell stage²¹. Different protein kinase C (PKC) isoforms, such as PKC- ϵ and PKC- δ , are critical for the proper assembly of ZO proteins and occludins²². At this stage, the apicobasal polarity does not require a basement membrane but is critically dependent on cell contact

asymmetry in the outer cells of the blastula²³. E-cadherin is also essential in this process, as E-cadherin homozygous null mutants fail to form a blastocoelic cavity²⁴. Despite evidence for cadherin switching in other tissues, E-cadherin cannot be substituted by N-cadherin to create a functional trophectodermal epithelial layer during blastocoelic cavity formation²⁵. Between embryonic day 3.0 (E3.0) and E4.5, calcium-dependent, immature desmosomes shift to a calcium-independent, hyperadhesive state, under the control of PKC- α and PKC- β ²⁶. Most notably, the AP-2- γ transcription factor is essential for the formation of the first epithelium of the mouse embryo, as its gene inactivation results in the disappearance of tight junctions²⁷. Specifically, AP-2- γ induces polarity genes, such as *Pard6b*, and tight junction components, such as claudin-4 and claudin-6, tight junction protein 2, aquaporin-3 and sodium-potassium ATPase1b1 (ref. ²⁷). By contrast, other components of the polarity complex and tight junctions are downregulated.

Primitive endoderm. A second MET occurs to generate the primitive epithelial endoderm. Progenitor cells of this transient epithelial structure appear stochastically in the ICM at the 8-cell to 16-cell stage before the cells segregate at the 64-cell stage to establish an outer epithelial layer²⁸ (Fig. 1). This segregation is driven by the fibroblast growth factor 4 (FGF4)–FGF receptor 2 signalling axis, promoting extracellular signal-regulated kinase and GATA6 responses²⁸. Atypical PKC (aPKC) is expressed apically in this newly formed cell layer²². The primitive endoderm expresses tight junction components but undergoes partial EMT at its edges to form the parietal endoderm, which lines the basal surface of the trophectoderm²⁹. The primitive endoderm also gives rise to the visceral endoderm, which acquires epithelial cell polarity, including the expression of tight junction components³⁰.

Epiblast. The epiblast is the epithelial cell layer that gives rise to the embryo proper following gastrulation. How the epiblast is formed from the ICM through MET has been analysed in great detail³¹. Although ICM cells express E-cadherin at E3.5 at the time of blastocoelic cavity formation, they acquire the characteristic features of fully polarized cells only gradually²³ (Fig. 1). At the peri-implantation stage (E4.5), the ICM cells adopt a rosette-like structure, creating a lumen through hollowing rather than through cavitation²³. Subsequent early polarization events involve aPKC and Par6 accumulation at the centre of the rosette, accompanied by the basal localization of the nucleus, the subapical localization of the Golgi and the accumulation of the actomyosin contractile machinery apically along adherens junctions²³. By E5.0, a lumen enlarges through the repulsive interactions of the negatively charged podocalyxin expressed on the apical domain²³. A similar mechanism operates slightly later in the adjacent trophectoderm-derived extraembryonic ectoderm. During the post-implantation stage (E5.5), the two lumens merge as the embryo elongates to adopt a cup shape that gives rise to the proamniotic cavity. Polarization is induced by β_1 -integrin signalling, which interacts with the basement membrane assembled by the trophectoderm and the primitive endoderm surrounding the ICM²³. Epiblast cell polarity is maintained until primitive streak formation²³; this is the site of EMT and migration of mesodermal and definitive endodermal cells. During gastrulation and neurulation, the epiblast—now called the ectoderm—undergoes intense morphogenetic movements^{10,32}. Studies carried out in mouse embryos have revealed that the epiblast cells lining the primitive streak are protected from ingressing³³. In these cells, EMT induction is abolished following glycosylation of members of the thrombospondin type-1 repeat superfamily by O-fucosyl transferase 2 (ref. ³³). In chick embryos, dissociation of epiblast cells adjacent to the primitive streak is prevented by the Net1 RhoA guanine exchange factor, contributing to the maintenance of a microtubule network on the basal side and preserving the epiblast basement

membrane³⁴. During gastrulation, newly formed mesenchymal cells migrate rostrally and laterally and subsequently form transient epithelia through MET³⁵. Mesenchymal cells near the neural axis establish the paraxial mesoderm, which will form the epithelial structure of the somites³⁵. More laterally, mesenchymal cells regroup into transient epithelial-like structures of the intermediate and lateral mesoderm³⁵. We briefly describe these structures undergoing MET.

Paraxial mesoderm. Rho family small GTPases play important roles in MET during somite formation. In the mesenchymal paraxial mesoderm, cell division cycle protein 42 (Cdc42) and Rac1 must remain expressed at intermediate levels, otherwise the somitic epithelium becomes aberrantly organized³⁶. Rac1 contributes to the induction of somitogenesis by acting post-transcriptionally on the basic-loop-helix transcription factor paraxis³⁶.

Intermediate mesoderm. Kidney development is another striking example of the importance of MET³⁷. Cells close to the paraxial mesoderm establish the intermediate mesoderm, a separate structure along the dorsoventral axis. The definitive kidney, known as the metanephros, derives from the caudal region of the intermediate mesoderm. The caudal intermediate mesodermal region originates from mesenchymal mesodermal cells of the late gastrulating epiblast cells at the primitive streak. The intermediate mesoderm initially contains all the cells that will give rise to the metanephros. However, the intermediate mesoderm becomes segregated into two structures: the epithelial nephric duct and the metanephric mesenchyme. The kidney forms through the reciprocal interaction of the lateral buds from the nephric duct, called the ureteric bud, which induces MET in the adjacent nephric mesenchyme. In turn, this mesenchyme induces branching morphogenesis in the ureteric bud, with lateral branching induced by glial-cell-derived neurotrophic factor. Some mesenchymal metanephric cells, called cap cells, undergo MET to form a connected renal vesicle, a transient structure that first adopts a comma-shape, then an S-shape, before giving rise to part of the glomerulus³⁷. Cells of the renal vesicle closer to the ureteric bud will form the proximal tubule, the loop of Henle and the distal tubule to create the mature nephron³⁸. MET in the cap mesenchyme is induced by Wnt9b, which is expressed by the ureteric bud³⁹. Wnt9b stabilizes β -catenin and represses the sine oculis homeobox 2 transcription factor and Cbp/p300-interacting transactivator 1 to engage cap cells into renal epithelial differentiation. This induction can be partially reproduced in vitro: human ESCs are first induced into mesenchymal cells using glycogen synthase kinase 3 (GSK3) inhibitors or high bone morphogenetic protein 4 (BMP4) and low activin A concentrations, thereby mimicking gastrulation. They are then induced to form the intermediate mesoderm through FGF9 stimulation, followed by the formation of the ureteric bud and metanephric mesenchyme, with an island of renal vesicles seen in two-dimensional (2D) cultures and nephrons in organoid cultures⁴⁰.

Lateral mesoderm. At the trunk level, the lateral mesenchyme undergoes MET to form two distinct transient epithelial layers—the somatopleure and the splanchnopleure—and undergoes hollowing to generate the coelomic cavity⁴¹. More rostrally, mesenchymal cells that are destined to form heart cell progenitors are incorporated into two symmetrical crescents in the splanchnopleural mesoderm. The myocardial progenitor cells specified before gastrulation acquire their restricted potential when the heart tube starts shaping through folding of the two lateral domains of the heart field. The inner layer of the splanchnopleure will then undergo EMT to generate endothelial progenitors, which will subsequently form the endocardium through MET. These two concentric epithelial-like structures—the myocardium and the endocardium—now constitute the heart tube. However, a second wave of progenitor cells that originate from the

secondary heart field will also contribute to the heart through a similar process, except that the endocardium originates from a domain that is distinct to that of the myocardium^{42,43}. Despite the efforts to unravel the mechanisms controlling the specification, determination and differentiation of these two components of the heart, we do not have mechanistic insight regarding MET in these tissues, in contrast to our knowledge on EMT in the endocardium during valve formation⁴⁴.

MET is also involved in the formation of the epicardium. This single-layered epithelium originates from sinus venosus mesenchymal cells, which migrate and subsequently undergo MET at the external surface of the myocardium⁴⁴. The zinc-finger Wilms tumour transcription factor, WT1, controls this MET but is also involved in an EMT programme in the epicardium^{45,46}.

Endoderm. The definitive endoderm formed during gastrulation becomes regionalized along the rostral–caudal axis to develop the lung, pancreas and liver. Here, we present the liver as an example of endoderm-derived organogenesis through cycles of EMT and MET. Gastrulating cells at the source of the definitive endoderm undergo EMT before inserting into the primitive endoderm (hypoblast) through MET³⁵. A small area of the closing foregut endoderm becomes specified to hepatic lineages through its proximity to the heart rudiment, secreting FGF family members⁴⁷. Endodermal cells that form the hepatic buds migrate into the surrounding mesenchyme (the septum transversum), which contributes to specification and promotes EMT in the hepatic bud through the GATA4-mediated induction of BMP4 and the resulting downregulation of E-cadherin⁴⁸. Hepatoblasts invade the septum transversum, driven by prospero homeobox 1 (*PROX1*), a target gene of the T-box transcription factor TBX3, before undergoing MET to initiate liver morphogenesis^{47,49}. TBX3 also induces and maintains hepatocyte nuclear factor 4- α (HNF4- α) and CCAAT/enhancer-binding protein- α (C/EBP- α) in hepatoblasts and inhibits HNF1- β and HNF6, which are critical for the formation of the cholangiocyte lineage⁵⁰. MET in hepatoblasts leads to the differentiation and assembly of hepatocytes into cords and to differentiation into cholangiocytes, forming bile ducts. However, quite remarkably and in contrast to cholangiocytes and the periportal hepatocytes, which express E-cadherin at the adult stage, the perivenous hepatocytes express N-cadherin⁵¹. Periportal hepatocytes and intrahepatic cholangiocytes may be exposed to a similar microenvironment that favours E-cadherin expression. However, these hepatoblast-derived cell types differ considerably. Whereas hepatocytes exhibit a unique polarization to construct the bile canaliculus by abutting two apical domains that are sealed by tight junctions, adherens junctions and desmosomes⁵², cholangiocytes organize a tubular structure lined by a single, polarized, E-cadherin-expressing cell layer⁵³.

Building polarity in epithelia. How MET is executed has been partly elucidated by studying apicobasal polarity, a complex programme coupled with lumen formation and regulated by a set of proteins and lipids, including Rho GTPases, polarity complex proteins^{54,55} and phosphoinositides^{56,57}. Polarization is initiated by cues from intercellular adhesion and interactions with the extracellular matrix (ECM), which are mediated primarily through integrins^{58,59}. Dystroglycans, another type of ECM receptor, are also implicated in basement membrane assembly and cell polarity^{60–65}. RhoA, its effector Rho-associated kinase 1 and myosin II also play crucial roles in orienting cell polarity by regulating actomyosin contractility^{66,67}. Once the apicobasal axis is established, cortical actin becomes contractile⁶⁸, coordinating Rab-GTPase-mediated polarized endosomal trafficking to create the lumen at cell–cell contacts, the enlargement of which is controlled by cell division⁶⁹. As in epiblast formation, lumen formation after membrane separation at the putative apical

cell–cell contact is called ‘hollowing’ and is considered part of the MET mechanism.

Polarization generates the apical membrane, which faces the lumen, and the basolateral membrane, which ensures intercellular adhesion and interaction with the ECM^{69,70} (Fig. 2). Intercellular adhesion is established through the formation of cell–cell junctions, including tight junctions, adherens junctions, desmosomes and gap junctions, along the lateral membrane^{2,4}.

E-cadherin clusters form in neighbouring cells through cis- and trans-interactions^{71,72}. Downstream signalling events are initiated by E-cadherin binding to β -catenin, which interacts with α -catenin to indirectly recruit Rac, Rho and their effectors, thereby promoting the formation and stabilization of the cortical actin network, which in turn strengthens adherens junctions^{71,73–75}. Members of the nectin family also contribute to the establishment of adherens junctions through cell–cell and cell–ECM crosstalk and are required for lumen formation^{68,76,77}.

Three evolutionarily conserved protein complexes are localized along the apicobasal axis. The Crumbs complex, at the apical domain, comprises Crumbs, protein-associated with Lin seven 1 (PALS1) and PALS1-associated tight junction protein (PATJ)⁷⁸. The Par complex, consisting of Par3, Par6 and aPKC, accumulates at tight junctions, whereas the Scribble complex, comprising Scribble, discs large (Dlg) and lethal giant larvae (Lgl), localizes at the basolateral membrane⁷⁸. The identity and boundaries (or size) of the apical and basolateral domains are established through repressive and cooperative interactions between these different complexes and through the actions of adherens junction proteins^{54,55}. Par3 has been primarily associated with the formation and stabilization of ZO-1-containing tight junctions, but was recently shown to also regulate the formation and stability of adherens junctions⁷⁶. Upstream of the Par complex are Rac1 and Cdc42, which contribute to the activation of aPKC^{79–81}. aPKC phosphorylates several polarity proteins, including Crumbs⁸², Lgl^{83–85} and GSK3- β ⁸⁶. Par3 associates with dynein and contributes to the local regulation of microtubule dynamics at cell–cell contacts and proper positioning of the centrosome at the cell centre^{87,88} and controls actin dynamics by regulating Rac1⁸⁹. Par3 also binds to the Rac guanine exchange factor Tiam1 to inhibit its activity and thereby suppress Rac1⁸⁹. By inhibiting Rac1 signalling and its protrusive activity at nascent cell–cell contacts, Par3 promotes a switch to Rho signalling, leading to actin cable formation and the stabilization of adherens junctions^{76,90}. Par3 depletion in different systems can affect both tight junctions and adherens junctions. In mammalian cells, in which these junctions are in close proximity and share common assembly mechanisms, cross-interaction has been observed between the Scribble and Par complexes^{2,90}. A direct interaction between the Crumbs and Par complexes promotes tight junction assembly⁹¹.

Phosphoinositides also regulate polarity through their spatial restriction^{57,92,93} (Fig. 2). Phosphatase and tensin homologue (PTEN) generates phosphatidylinositol (4,5)-bisphosphate (PtdIns(4,5)P₂) from PtdIns(3,4,5)P₃; PtdIns(4,5)P₂, annexin 2 and activated Cdc42 are required for the targeting and localization of Par6 and PKC to the apical domain to regulate the formation of the apical plasma membrane and lumen during epithelial morphogenesis^{93,94}.

Although PTEN is unlikely to be the only regulator of PtdIns(4,5)P₂ during apical membrane specification, PtdIns(4,5)P₂ on the apical surface is mainly generated by the phosphorylation of PtdIns4P by PtdInsP 5-kinase, which selectively regulates apical endocytosis^{95,96}. SH2-domain-containing inositol 5-phosphatase 2 and its lipid product PtdIns(3,4)P₂ bind to Dlg homologue 1 (Dlg1) to stabilize the basolateral membrane⁹⁷ and regulate RhoA-dependent actin contractility and cell division to create the lumen⁹⁸ (Fig. 2). Phosphatidylinositol-3-OH kinase (PI3K) also controls the organization of epithelial cells by restricting liver kinase B1 signalling both

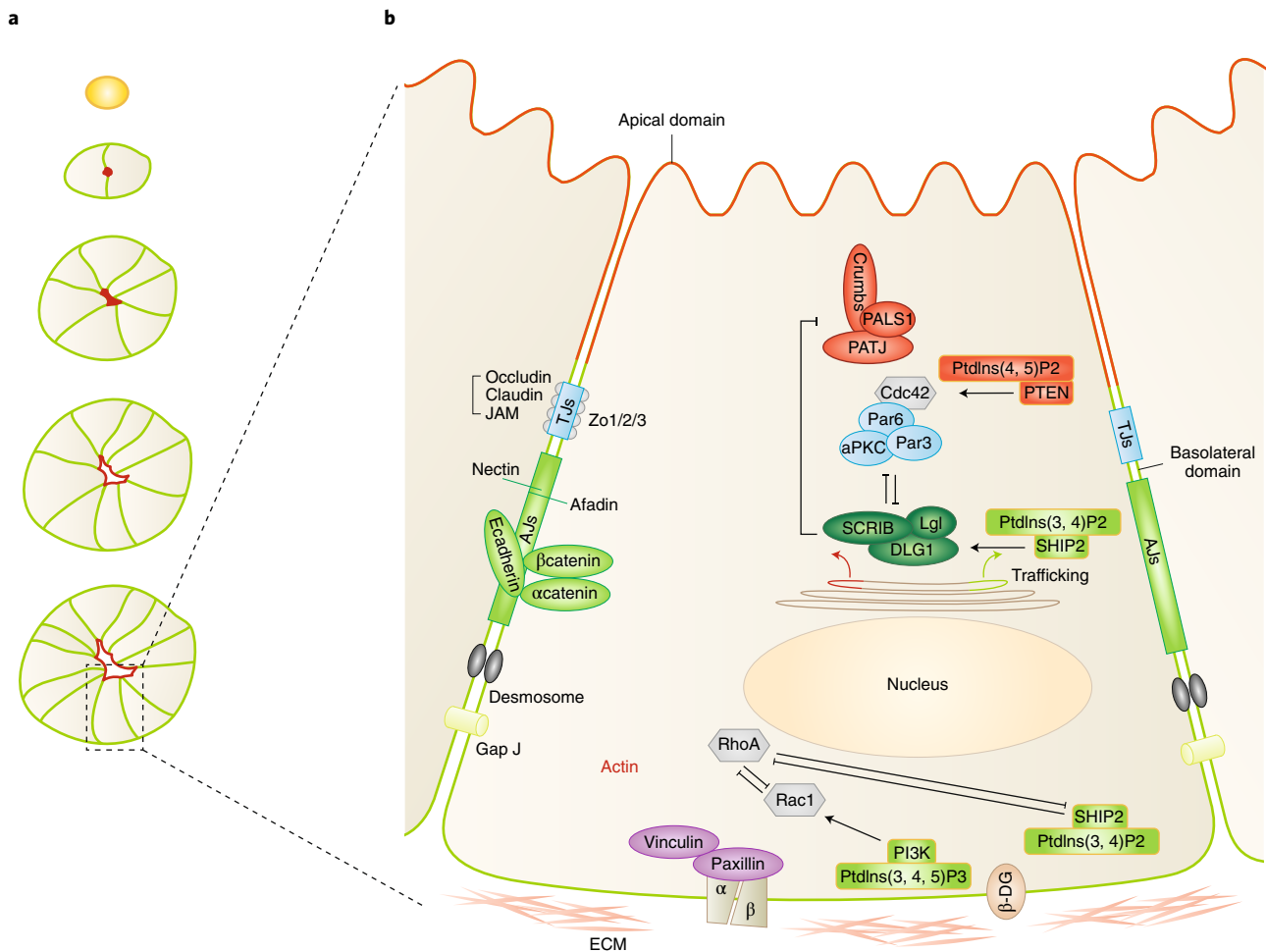


Fig. 2 | Determinants of apicobasal polarity and lumen formation in epithelial cells. During epithelial morphogenesis, the establishment of apicobasal polarity and lumen formation are controlled by polarity protein complexes, phosphoinositides and signalling pathways. **a**, The mechanisms of lumen formation have been elucidated primarily using 3D *in vitro* cultures of epithelial cells. Apical proteins (red) start to accumulate at the centre of cell doublets cultured in Matrigel, whereas cell-cell contacts are devoid of β -catenin (green). The lumen develops a pre-apical patch and becomes enlarged concurrently with cell division¹⁴⁸. The polarized epithelial cells form a mature cyst, where a central lumen is surrounded by a monolayer of tightly associated cells. **b**, The plasma membrane of polarized epithelial cells comprises a basolateral membrane containing adherens junctions (AJs) and is associated with the basement membrane and the ECM. Tight junctions (TJs) separate the lumen-facing apical membranes (red line) from the basolateral membrane (green line). Polarity complexes are distributed asymmetrically along the apicobasal axis. The Crumbs complex (red), consisting of Crumbs, PALS1-associated tight junction protein (PATJ) and PALS1, localizes to the apical membrane. The Par complex (blue), which is composed of aPKC, Par3 and Par6, is located laterally where it interacts with tight junctions. Scribble, Lgl and Dlg comprise the Scribble complex (dark green) at the basolateral surface. Phosphoinositides and their metabolizing enzymes (rectangles outlined in yellow) are polarized and have specific subcellular localizations. PtdIns(4,5)P₂ (red) is enriched at the apical membrane, whereas PtdIns(3,4)P₂ and PtdIns(3,4,5)P₃ (dark green) are enriched at the basolateral surface. PTEN is activated at the apical pole to generate PtdIns(4,5)P₂ and mediate lumen formation. SH2-domain-containing inositol 5-phosphatase 2 (SHIP2) produces PtdIns(3,4)P₂ at the basal pole and stabilizes polarity complex proteins such as Dlg homologue 1 (DLG1) or Scribble, which support epithelial architecture. Membrane trafficking from the Golgi ensures the correct targeting to the apical surface or the basolateral surface. β -DG, β -dystroglycan; JAM, junctional adhesion molecule. Figure adapted from ref. ¹⁴⁹.

in *Drosophila* and in mammalian epithelial cells in 3D culture⁹⁹. PtdIns(3,4,5)P₃, produced by the δ -isoform of PI3K (PI3K- δ) and enriched on the basolateral surface, orients the apicobasal axis, participates in building the basolateral membrane and lumen formation through ECM assembly^{100,101}.

Collectively, these data reveal the dynamic and elaborate cross-talk between polarity and junctional complexes, Rho GTPases and phosphoinositides for the establishment and stability of epithelial cell polarity, leading to the completion of MET.

MET in cell fate conversions and somatic cell reprogramming

Somatic cell reprogramming by a combination of Oct4, Sox2, Klf4 and Myc (hereafter OSKM factors)¹⁰² provides an ideal *in vitro* model to investigate the regulation of cell fate changes. Accumulating evidence indicates that MET is essential during early somatic cell reprogramming in mouse embryonic fibroblasts (MEFs) and human fibroblasts^{103,104}, and that blocking this step can impair reprogramming efficiency¹⁰⁵. In the initial stages of MEF reprogramming, Sox2, Oct4 and Myc suppress TGF- β -Snail

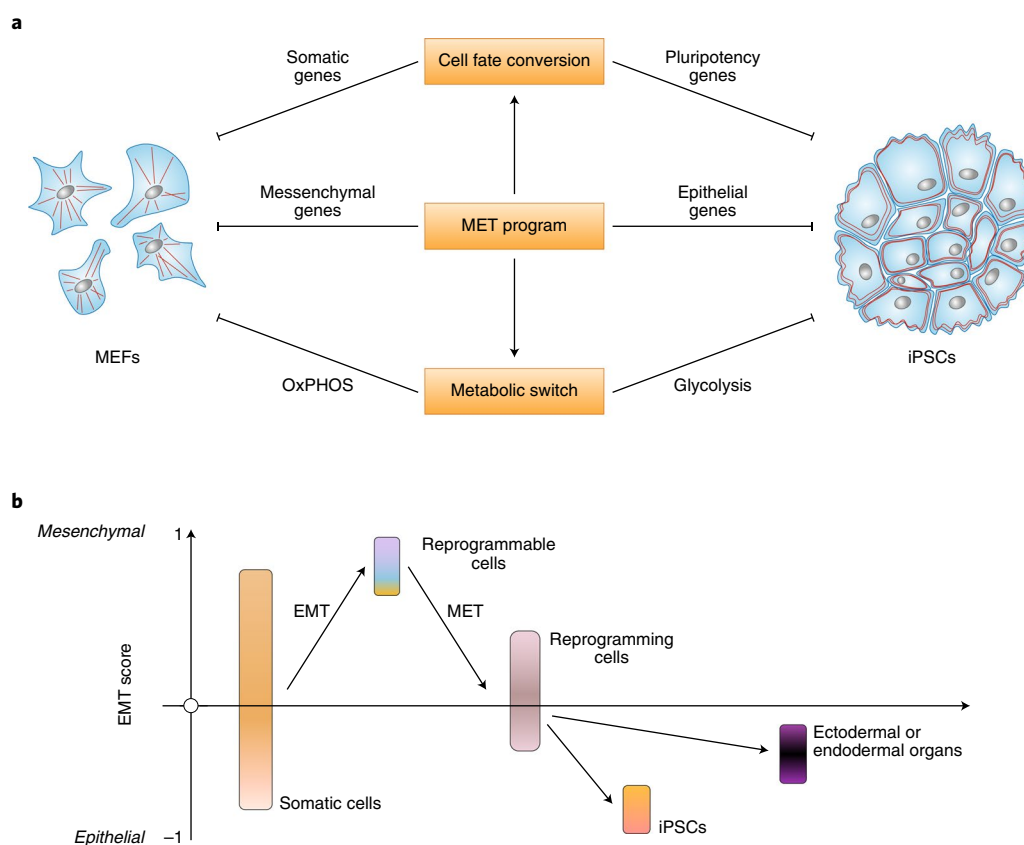


Fig. 3 | Sequential EMT and MET for reprogramming of somatic cells. a, Major changes in the somatic reprogramming of MEFs. The OSKM factors silence somatic genes in MEFs and induce pluripotency genes during the late stages of reprogramming. A metabolic switch from oxidative phosphorylation (OxPHOS) to glycolysis occurs during reprogramming. MET is an essential early step in reprogramming, as it remodels the mesenchymal cytoskeleton and cell-surface protein expression to adopt an epithelial-like morphology and facilitates metabolic and cell fate changes. **b**, Schematic outline of stemness acquisition in the EMT spectrum. Epithelial-like or mesenchymal-like somatic cells can be reprogrammed using OSKM factors and/or small molecules. The first step is to induce a quasi-mesenchymal phenotype, with stemness acquired during the early phase of MET¹²⁰, at which point cells can be reprogrammed into iPSCs or endodermal or ectodermal derivatives¹⁵⁰.

signalling, whereas Klf4 induces the epithelial programme¹⁰⁵, with a net effect of downregulating mesenchymal proteins and upregulating epithelial proteins, as confirmed by proteomics analyses¹⁰⁶ (Fig. 3a). BMP-driven MET can also facilitate reprogramming¹⁰⁷, as can the use of well-controlled MEF adhesion conditions, such as growth on microgrooved substrates or soft hydrogels^{108,109}. By contrast, dual specificity testis-specific protein kinase 1 and LIM domain kinase 2 (Limk2), which promote actin polymerization in fibroblasts, impede reprogramming¹¹⁰.

Recent studies indicate that MET-like changes are also involved in the reprogramming of other somatic cell types. For instance, mouse B cells can be reprogrammed into iPSCs by OSKM factors and the forced expression of C/EBP- α , leading to MET-like gene expression changes¹¹¹. MET is also observed when reprogramming haematopoietic progenitor and stem cells¹¹² and spermatogonial stem cells¹¹³, with an active mesenchymal programme functioning as a reprogramming barrier. MEFs from the Tet1/2/3 triple-knock-out mice failed to be reprogrammed into iPSCs due to a failure to undergo MET¹¹⁴. Intriguingly, however, more epithelial-like neural progenitor cells and keratinocytes from the same mice could be reprogrammed efficiently in the same study. These data clearly demonstrate that the acquisition of an epithelial-like status is a prerequisite for cells to establish pluripotency.

In addition to iPSCs, MEFs can be directly converted into other epithelial-like cells, such as induced hepatocyte-like cells, by the

overexpression of transcription factors, such as Myc and Klf4, and/or through treatment with small molecules^{115–117}. In the chemical-induced conversion of MEFs into hepatocytes, cells first undergo MET to become endodermal progenitors and then further differentiate into cells of the hepatic lineage¹¹⁸. Similar transitions between epithelial and mesenchymal statuses are observed in the hepatic differentiation of ESCs in vitro: ESCs are epithelial cells and an EMT event occurs during ESC differentiation into the definitive endoderm, whereas MET takes place at later stages of hepatic differentiation and maturation^{119,120}. In vitro hepatic differentiation mimics in vivo liver development, with a round of EMT–MET involved in the acquisition of hepatic cell fate.

Somatic cell reprogramming studies show that an epithelial or mesenchymal status of the cell at the beginning of induction affects iPSC generation. For example, pre-treatment of MEFs with the TGF- β receptor inhibitor RepSox reduces the efficiency of OSKM-induced reprogramming^{121,122}. By contrast, TGF- β pre-treatment drives MEFs to a more mesenchymal state and enhances reprogramming efficiency¹²¹. In the same study, the sequential introduction of OSKM showed that an initial EMT is beneficial for subsequent MET in MEF reprogramming. In B cells, C/EBP- α treatment induces an EMT and promotes the efficiency of OSKM-mediated reprogramming¹¹¹. It is possible that EMT as the initial step may synchronize and prime cells for reprogramming, although this remains to be formally demonstrated.

Epigenetic status also determines the capacity of somatic cells for iPSC reprogramming. Dynamic epigenetic changes occur during reprogramming, including DNA methylation and histone modifications¹²³, and MET events are also under epigenetic control^{114,124–126}. For example, the failure of MEFs from Tet1/2/3 triple-knockout mice to be reprogrammed stems from disrupted DNA demethylation¹¹⁴; conversely, the histone H3K36 demethylases Kdm2a/2b enhance reprogramming, at least partially, through the promotion of MET at the initial stages^{124,126}. Furthermore, blocking the H3K79 methyltransferase DOT1L downregulates mesenchymal gene expression and enhances reprogramming efficiency¹²⁵.

In addition to MET-type morphological changes, successful iPSC reprogramming from MEFs requires a metabolic switch. Whereas mesenchymal cells, such as MEFs, rely more on oxidative phosphorylation and mitochondrial functions, pluripotent stem cells, including ESCs and iPSCs, require high glycolysis levels^{13,127} and rely on distinct metabolic pathways to maintain pluripotency-related epigenetic modifications (Fig. 3a). For example, a threonine catabolic pathway supplies S-adenosylmethionine, which is essential for H3K4 methylation and the maintenance of pluripotency in mouse ESCs¹²⁸. The methionine–S-adenosylmethionine pathway functions in a similar manner in human ESCs or iPSCs¹²⁹. α -Ketoglutarate, a metabolite of the tricarboxylic acid cycle, also contributes to the maintenance of mouse ESCs through histone and DNA demethylation¹³⁰. Acetyl-CoA, a product of glycolysis, promotes histone acetylation and maintains ESC pluripotency¹³¹. Defects in these metabolic pathways can disrupt pluripotency and result in differentiation^{128–131}. Thus, a MET-induced metabolic switch during reprogramming may promote global epigenetic modifications that favour either the establishment or the maintenance of pluripotency.

Concluding remarks

Early in embryogenesis, the formation and plasticity of an epithelial anlage allow cells to engage in EMT for the execution of morphogenetic events during gastrulation and organogenesis. Most of these cells will re-acquire intercellular adhesion at the onset of MET to generate different epithelial organizations³⁵. However, some mesenchymal cells will never revert to an epithelial state¹³². Similarly, reprogramming somatic cells into iPSCs transiently involves a full EMT to reset the epigenetic landscape, followed by MET to acquire stemness. The transition to the stem-like state probably occurs at an intermediate EMT state before all epithelial traits are acquired¹²⁰ (Fig. 3b).

Mechanisms driving epithelial apicobasal polarity have been partially elucidated and provide an understanding of the principles driving morphological organization in early-stage embryos and in adult tissues. One critical issue is the precise estimation of ‘mesenchymality’ in any cell type of the body. This is technically challenging but already feasible in several tissues^{3,133}. Surprisingly, epithelial tissues exhibit a range of EMT scores, with the colon being more epithelial like and the kidney more mesenchymal like. The EMT spectrum of these epithelial tissues is somewhat reflected by the average value of EMT scores in carcinoma cell lines and tumours originating from the same tissues¹³⁴.

Several avenues of research could identify the factors that strengthen the stability of epithelia. Such factors could prevent or revert the partial EMT phenotype acquired by epithelial cells of the kidney^{135,136} and other organs in fibrotic disease¹. However, inhibiting MET can also be beneficial, as in the case of granuloma formed by aggregated macrophages that mask parasites or infectious bacteria¹³⁷. Quite surprisingly, these macrophages acquire an epithelial-like phenotype through the expression of E-cadherin, leading to adherens junction formation. Disrupting such aggregates could be beneficial against chronic infections that are resistant to antibiotics or antiparasitic drugs, such as in tuberculosis and schistosomiasis¹³⁷. A beneficial effect may also be expected in carcinoma, given that

mesenchymal-like carcinoma cells are more prone to metastasis^{6,138} and are more refractory to chemotherapy and targeted therapeutics¹. In addition, MET can suppress tumour-initiating cells^{139,140}, which may improve patient responses to antimetabolic drugs. Most importantly, cytotoxic T lymphocytes cannot develop a functional immunological synapse in epithelial carcinoma cells acquiring a mesenchymal-like phenotype by EMT inducers. Cytotoxicity can be restored in these mesenchymal-like carcinoma cells that are rendered more epithelial like using MET inducers, such as the TGF- β receptor inhibitor A83.01 (refs ^{141–143}). Recently, AXL was found to form a multimolecular complex with other receptor tyrosine kinases in ovarian carcinoma cells exhibiting a mesenchymal phenotype¹⁴⁴. MET can be induced by the AXL inhibitor R428 (ref. ¹⁴⁴), which abrogates tumour growth. A complementary strategy would be to leverage the fact that a mesenchymal status confers sensitivity to ferroptosis, an oxidative form of iron-dependant cell death mediated by lipid hydroperoxides¹⁴⁵. Glutathione peroxidase 4 has been identified as a critical suppressor of ferroptosis by reducing the levels of allylic lipid hydroperoxides^{146,147}. Drugs targeting glutathione peroxidase 4 will potentially contribute to eradicate refractory mesenchymal-like carcinoma or sarcoma cells in tumours¹⁴⁶.

Considering the high research activity in the field of epithelial and mesenchymal transitions, we can expect that in the coming years, we will witness the discovery of more regulators that maintain the epithelial state and the further elucidation of the mechanisms driving MET in embryonic development and cancer, to facilitate the development of new therapeutic strategies.

Received: 25 January 2018; Accepted: 10 August 2018;
Published online: 2 January 2019

References

- Nieto, M. A., Huang, R. Y., Jackson, R. A. & Thiery, J. P. EMT: 2016. *Cell* **166**, 21–45 (2016).
- Rodriguez-Boulant, E. & Macara, I. G. Organization and execution of the epithelial polarity programme. *Nat. Rev. Mol. Cell Biol.* **15**, 225–242 (2014).
- Dong, J. et al. Single-cell RNA-seq analysis unveils a prevalent epithelial/mesenchymal hybrid state during mouse organogenesis. *Genome Biol.* **19**, 31 (2018).
- Huang, R. Y., Guilford, P. & Thiery, J. P. Early events in cell adhesion and polarity during epithelial–mesenchymal transition. *J. Cell Sci.* **125**, 4417–4422 (2012).
- Lim, J. & Thiery, J. P. Epithelial–mesenchymal transitions: insights from development. *Development* **139**, 3471–3486 (2012).
- Pastushenko, I. et al. Identification of the tumour transition states occurring during EMT. *Nature* **556**, 463–468 (2018).
- Tepass, U. Epithelial differentiation in *Drosophila*. *Bioessays* **19**, 673–682 (1997).
- Tepass, U. & Hartenstein, V. The development of cellular junctions in the *Drosophila* embryo. *Dev. Biol.* **161**, 563–596 (1994).
- Campbell, K., Casanova, J. & Skaer, H. Mesenchymal-to-epithelial transition of intercalating cells in *Drosophila* renal tubules depends on polarity cues from epithelial neighbours. *Mech. Dev.* **127**, 345–357 (2010).
- Stern, C. D. (ed.). *Gastrulation: From Cells to Embryos* (Cold Spring Harbor Laboratory Press, New York, 2004).
- Varga, J. & Gretchen, F. R. Cell plasticity in epithelial homeostasis and tumorigenesis. *Nat. Cell Biol.* **19**, 1133–1141 (2017).
- Shu, X. & Pei, D. The function and regulation of mesenchymal-to-epithelial transition in somatic cell reprogramming. *Curr. Opin. Genet. Dev.* **28**, 32–37 (2014).
- Wu, J., Ocampo, A. & Belmonte, J. C. I. Cellular metabolism and induced pluripotency. *Cell* **166**, 1371–1385 (2016).
- Loubat-Casanovas, J. et al. Snail1 is required for the maintenance of the pancreatic acinar phenotype. *Oncotarget* **7**, 4468–4482 (2016).
- Chakrabarti, R. et al. EMT5 inhibits the epithelial–mesenchymal transition in mammary gland development and breast cancer metastasis by transcriptionally repressing Snail2. *Nat. Cell Biol.* **14**, 1212–1222 (2012).
- Ray, H. J. & Niswander, L. A. Grainyhead-like 2 downstream targets act to suppress epithelial-to-mesenchymal transition during neural tube closure. *Development* **143**, 1192–1204 (2016).
- Chung, V. Y. et al. GRHL2–miR-200–ZEB1 maintains the epithelial status of ovarian cancer through transcriptional regulation and histone modification. *Sci. Rep.* **6**, 19943 (2016).

18. Frisch, S. M., Farris, J. C. & Pifer, P. M. Roles of Grainyhead-like transcription factors in cancer. *Oncogene* **36**, 6067–6073 (2017).
19. Lee, B. et al. Transcriptional mechanisms link epithelial plasticity to adhesion and differentiation of epidermal progenitor cells. *Dev. Cell* **29**, 47–58 (2014).
20. Watanabe, K. et al. Mammary morphogenesis and regeneration require the inhibition of EMT at terminal end buds by *Ovol2* transcriptional repressor. *Dev. Cell* **29**, 59–74 (2014).
21. Eckert, J. J. & Fleming, T. P. Tight junction biogenesis during early development. *Biochim. Biophys. Acta* **1778**, 717–728 (2008).
22. Eckert, J. J. et al. Relative contribution of cell contact pattern, specific PKC isoforms and gap junctional communication in tight junction assembly in the mouse early embryo. *Dev. Biol.* **288**, 234–247 (2005).
23. Bedzhov, I. & Zernicka-Goetz, M. Self-organizing properties of mouse pluripotent cells initiate morphogenesis upon implantation. *Cell* **156**, 1032–1044 (2014).
24. Larue, L., Ohsugi, M., Hirschenhain, J. & Kemler, R. E-cadherin null mutant embryos fail to form a trophectoderm epithelium. *Proc. Natl Acad. Sci. USA* **91**, 8263–8267 (1994).
25. Kan, N. G. et al. Gene replacement reveals a specific role for E-cadherin in the formation of a functional trophectoderm. *Development* **134**, 31–41 (2007).
26. Kimura, T. E. et al. Desmosomal adhesiveness is developmentally regulated in the mouse embryo and modulated during trophectoderm migration. *Dev. Biol.* **369**, 286–297 (2012).
27. Choi, I., Carey, T. S., Wilson, C. A. & Knott, J. G. Transcription factor *AP-2γ* is a core regulator of tight junction biogenesis and cavity formation during mouse early embryogenesis. *Development* **139**, 4623–4632 (2012).
28. Hermitte, S. & Chazaud, C. Primitive endoderm differentiation: from specification to epithelium formation. *Phil. Trans. R. Soc. B* **369**, 20130537 (2014).
29. Veltmaat, J. M. et al. Snail is an immediate early target gene of parathyroid hormone related peptide signaling in parietal endoderm formation. *Int. J. Dev. Biol.* **44**, 297–307 (2000).
30. Phua, D. C. et al. ZO-1 and ZO-2 are required for extra-embryonic endoderm integrity, primitive ectoderm survival and normal cavitation in embryoid bodies derived from mouse embryonic stem cells. *PLoS ONE* **9**, e99532 (2014).
31. Artus, J. & Chazaud, C. A close look at the mammalian blastocyst: epiblast and primitive endoderm formation. *Cell. Mol. Life Sci.* **71**, 3327–3338 (2014).
32. Sokol, S. Y. Mechanotransduction during vertebrate neurulation. *Curr. Top. Dev. Biol.* **117**, 359–376 (2016).
33. Du, J. et al. O-fucosylation of thrombospondin type 1 repeats restricts epithelial to mesenchymal transition (EMT) and maintains epiblast pluripotency during mouse gastrulation. *Dev. Biol.* **346**, 25–38 (2010).
34. Nakaya, Y., Sukowati, E. W., Wu, Y. & Sheng, G. RhoA and microtubule dynamics control cell-basement membrane interaction in EMT during gastrulation. *Nat. Cell Biol.* **10**, 765–775 (2008).
35. Gilbert, S. F. & Barresi, M. J. F. *Developmental Biology* (Sinauer Associates, Oxford, 2016).
36. Nakaya, Y., Kuroda, S., Katagiri, Y. T., Kaibuchi, K. & Takahashi, Y. Mesenchymal–epithelial transition during somitic segmentation is regulated by differential roles of *Cdc42* and *Rac1*. *Dev. Cell* **7**, 425–438 (2004).
37. Costantini, F. & Kopan, R. Patterning a complex organ: branching morphogenesis and nephron segmentation in kidney development. *Dev. Cell* **18**, 698–712 (2010).
38. Takasato, M. & Little, M. H. The origin of the mammalian kidney: implications for recreating the kidney in vitro. *Development* **142**, 1937–1947 (2015).
39. Carroll, T. J., Park, J. S., Hayashi, S., Majumdar, A. & McMahon, A. P. *Wnt9b* plays a central role in the regulation of mesenchymal to epithelial transitions underlying organogenesis of the mammalian urogenital system. *Dev. Cell* **9**, 283–292 (2005).
40. Takasato, M. et al. Directing human embryonic stem cell differentiation towards a renal lineage generates a self-organizing kidney. *Nat. Cell Biol.* **16**, 118–126 (2014).
41. Abu-Issa, R. & Kirby, M. L. Heart field: from mesoderm to heart tube. *Annu. Rev. Cell Dev. Biol.* **23**, 45–68 (2007).
42. Meilhac, S. M., Lescroart, F., Blainpain, C. & Buckingham, M. E. Cardiac cell lineages that form the heart. *Cold Spring Harb. Perspect. Med.* **4**, a013888 (2014).
43. Tirosh-Finkel, L., Elhanany, H., Rinon, A. & Tzahor, E. Mesoderm progenitor cells of common origin contribute to the head musculature and the cardiac outflow tract. *Development* **133**, 1943–1953 (2006).
44. von Gise, A. & Pu, W. T. Endocardial and epicardial epithelial to mesenchymal transitions in heart development and disease. *Circ. Res.* **110**, 1628–1645 (2012).
45. Asli, N. S. & Harvey, R. P. Epithelial to mesenchymal transition as a portal to stem cell characters embedded in gene networks. *Bioessays* **35**, 191–200 (2013).
46. Moore, A. W., McInnes, L., Kreidberg, J., Hastie, N. D. & Schedl, A. YAC complementation shows a requirement for *Wt1* in the development of epicardium, adrenal gland and throughout nephrogenesis. *Development* **126**, 1845–1857 (1999).
47. Si-Tayeb, K., Lemaigre, F. P. & Duncan, S. A. Organogenesis and development of the liver. *Dev. Cell* **18**, 175–189 (2010).
48. Bort, R., Signore, M., Tremblay, K., Martinez Barbera, J. P. & Zaret, K. S. Hex homeobox gene controls the transition of the endoderm to a pseudostratified, cell emergent epithelium for liver bud development. *Dev. Biol.* **290**, 44–56 (2006).
49. Sosa-Pineda, B., Wigle, J. T. & Oliver, G. Hepatocyte migration during liver development requires *Prox1*. *Nat. Genet.* **25**, 254–255 (2000).
50. Ludtke, T. H., Christoffels, V. M., Petry, M. & Kispert, A. *Tbx3* promotes liver bud expansion during mouse development by suppression of cholangiocyte differentiation. *Hepatology* **49**, 969–978 (2009).
51. Doi, Y. et al. Development of complementary expression patterns of E- and N-cadherin in the mouse liver. *Hepatol. Res.* **37**, 230–237 (2007).
52. Tsukita, S. & Tsukita, S. Isolation of cell-to-cell adherens junctions from rat liver. *J. Cell Biol.* **108**, 31–41 (1989).
53. Tanimizu, N., Miyajima, A. & Mostov, K. E. Liver progenitor cells develop cholangiocyte-type epithelial polarity in three-dimensional culture. *Mol. Biol. Cell* **18**, 1472–1479 (2007).
54. Assemat, E., Bazellieres, E., Pallesi-Pocachard, E., Le Bivic, A. & Massey-Harroche, D. Polarity complex proteins. *Biochim. Biophys. Acta* **1778**, 614–630 (2008).
55. Bilder, D. Epithelial polarity and proliferation control: links from the *Drosophila* neoplastic tumor suppressors. *Genes Dev.* **18**, 1909–1925 (2004).
56. Gassama-Diagne, A. & Payrastra, B. Phosphoinositide signaling pathways: promising role as builders of epithelial cell polarity. *Int. Rev. Cell. Mol. Biol.* **273**, 313–343 (2009).
57. Krahn, M. P. & Wodarz, A. Phosphoinositide lipids and cell polarity: linking the plasma membrane to the cytocortex. *Essays Biochem.* **53**, 15–27 (2012).
58. Humphries, J. D., Byron, A. & Humphries, M. J. Integrin ligands at a glance. *J. Cell Sci.* **119**, 3901–3903 (2006).
59. Lee, J. L. & Streuli, C. H. Integrins and epithelial cell polarity. *J. Cell Sci.* **127**, 3217–3225 (2014).
60. Akhtar, N. & Streuli, C. H. An integrin–ILK–microtubule network orients cell polarity and lumen formation in glandular epithelium. *Nat. Cell Biol.* **15**, 17–27 (2013).
61. Bissell, M. J., Radisky, D. C., Rizki, A., Weaver, V. M. & Petersen, O. W. The organizing principle: microenvironmental influences in the normal and malignant breast. *Differentiation* **70**, 537–546 (2002).
62. Manninen, A. Epithelial polarity—generating and integrating signals from the ECM with integrins. *Exp. Cell Res.* **334**, 337–349 (2015).
63. Monteleon, C. L. et al. Establishing epithelial glandular polarity: interlinked roles for ARF6, Rac1, and the matrix microenvironment. *Mol. Biol. Cell* **23**, 4495–4505 (2012).
64. O'Brien, L. E. et al. *Rac1* orientates epithelial apical polarity through effects on basolateral laminin assembly. *Nat. Cell Biol.* **3**, 831–838 (2001).
65. Yu, W. et al. γ -integrin orients epithelial polarity via *Rac1* and laminin. *Mol. Biol. Cell* **16**, 433–445 (2005).
66. Bachir, A. I., Horwitz, A. R., Nelson, W. J. & Bianchini, J. M. Actin-based adhesion modules mediate cell interactions with the extracellular matrix and neighboring cells. *Cold Spring Harb. Perspect. Biol.* **9**, a023234 (2017).
67. Yu, W. et al. Involvement of RhoA, ROCK I and myosin II in inverted orientation of epithelial polarity. *EMBO Rep.* **9**, 923–929 (2008).
68. Ivanov, A. I. & Naydenov, N. G. Dynamics and regulation of epithelial adherens junctions: recent discoveries and controversies. *Int. Rev. Cell. Mol. Biol.* **303**, 27–99 (2013).
69. Overeem, A. W., Bryant, D. M. & van IJzendoorn, S. C. Mechanisms of apical–basal axis orientation and epithelial lumen positioning. *Trends Cell Biol.* **25**, 476–485 (2015).
70. Bryant, D. M. & Mostov, K. E. From cells to organs: building polarized tissue. *Nat. Rev. Mol. Cell Biol.* **9**, 887–901 (2008).
71. Engl, W., Arasi, B., Yap, L. L., Thiery, J. P. & Viasnoff, V. Actin dynamics modulate mechanosensitive immobilization of E-cadherin at adherens junctions. *Nat. Cell Biol.* **16**, 587–594 (2014).
72. Yap, A. S., Gomez, G. A. & Parton, R. G. Adherens junctions revisualized: organizing cadherins as nanoassemblies. *Dev. Cell* **35**, 12–20 (2015).
73. Acharya, B. R. & Yap, A. S. Pls Pls Pls: mechanochemical feedback and the morphogenetic role of contractility at cadherin cell–cell junctions. *Curr. Top. Dev. Biol.* **117**, 631–646 (2016).
74. Chu, Y. S. et al. Force measurements in E-cadherin-mediated cell doublets reveal rapid adhesion strengthened by actin cytoskeleton remodeling through *Rac* and *Cdc42*. *J. Cell Biol.* **167**, 1183–1194 (2004).
75. Lecuit, T. & Yap, A. S. E-cadherin junctions as active mechanical integrators in tissue dynamics. *Nat. Cell Biol.* **17**, 533–539 (2015).

76. Coopman, P. & Djiane, A. Adherens junction and E-cadherin complex regulation by epithelial polarity. *Cell. Mol. Life Sci.* **73**, 3535–3553 (2016).
77. Yang, Z. et al. De novo lumen formation and elongation in the developing nephron: a central role for afadin in apical polarity. *Development* **140**, 1774–1784 (2013).
78. St Johnston, D. & Ahringer, J. Cell polarity in eggs and epithelia: parallels and diversity. *Cell* **141**, 757–774 (2010).
79. Noda, Y. et al. Human homologues of the *Caenorhabditis elegans* cell polarity protein PAR6 as an adaptor that links the small GTPases Rac and Cdc42 to atypical protein kinase C. *Genes Cells* **6**, 107–119 (2001).
80. Qin, Y., Meisen, W. H., Hao, Y. & Macara, I. G. Tuba, a Cdc42 GEF, is required for polarized spindle orientation during epithelial cyst formation. *J. Cell Biol.* **189**, 661–669 (2010).
81. Qiu, R. G., Abo, A. & Steven Martin, G. A human homolog of the *C. elegans* polarity determinant Par-6 links Rac and Cdc42 to PKC ζ signaling and cell transformation. *Curr. Biol.* **10**, 697–707 (2000).
82. Sotillos, S., Diaz-Meco, M. T., Caminero, E., Moscat, J. & Campuzano, S. DaPKC-dependent phosphorylation of Crumbs is required for epithelial cell polarity in *Drosophila*. *J. Cell Biol.* **166**, 549–557 (2004).
83. Betschinger, J., Mechtler, K. & Knoblich, J. A. The Par complex directs asymmetric cell division by phosphorylating the cytoskeletal protein Lgl. *Nature* **422**, 326–330 (2003).
84. Dong, W. et al. A conserved polybasic domain mediates plasma membrane targeting of Lgl and its regulation by hypoxia. *J. Cell Biol.* **211**, 273–286 (2015).
85. Plant, P. J. et al. A polarity complex of mPar-6 and atypical PKC binds, phosphorylates and regulates mammalian Lgl. *Nat. Cell Biol.* **5**, 301–308 (2003).
86. Kim, M., Datta, A., Brakeman, P., Yu, W. & Mostov, K. E. Polarity proteins PAR6 and aPKC regulate cell death through GSK-3 β in 3D epithelial morphogenesis. *J. Cell Sci.* **120**, 2309–2317 (2007).
87. Chen, S. et al. Regulation of microtubule stability and organization by mammalian Par3 in specifying neuronal polarity. *Dev. Cell* **24**, 26–40 (2013).
88. Schmoranz, J. et al. Par3 and dynein associate to regulate local microtubule dynamics and centrosome orientation during migration. *Curr. Biol.* **19**, 1065–1074 (2009).
89. Chen, X. & Macara, I. G. Par-3 controls tight junction assembly through the Rac exchange factor Tiam1. *Nat. Cell Biol.* **7**, 262–269 (2005).
90. Matsuzawa, K. et al. PAR3–aPKC regulates Tiam1 by modulating suppressive internal interactions. *Mol. Biol. Cell* **27**, 1511–1523 (2016).
91. Hurd, T. W., Gao, L., Roh, M. H., Macara, I. G. & Margolis, B. Direct interaction of two polarity complexes implicated in epithelial tight junction assembly. *Nat. Cell Biol.* **5**, 137–142 (2003).
92. Schink, K. O., Tan, K. W. & Stenmark, H. Phosphoinositides in control of membrane dynamics. *Annu. Rev. Cell Dev. Biol.* **32**, 143–171 (2016).
93. Shewan, A., Eastburn, D. J. & Mostov, K. Phosphoinositides in cell architecture. *Cold Spring Harb. Perspect. Biol.* **3**, a004796 (2011).
94. Martin-Belmonte, F. et al. PTEN-mediated apical segregation of phosphoinositides controls epithelial morphogenesis through Cdc42. *Cell* **128**, 383–397 (2007).
95. Guerriero, C. J., Weixel, K. M., Bruns, J. R. & Weisz, O. A. Phosphatidylinositol 5-kinase stimulates apical biosynthetic delivery via an Arp2/3-dependent mechanism. *J. Biol. Chem.* **281**, 15376–15384 (2006).
96. Szalinski, C. M. et al. PIP5K β selectively modulates apical endocytosis in polarized renal epithelial cells. *PLoS ONE* **8**, e53790 (2013).
97. Awad, A. et al. SHIP2 regulates epithelial cell polarity through its lipid product, which binds to Dlg1, a pathway subverted by hepatitis C virus core protein. *Mol. Biol. Cell* **24**, 2171–2185 (2013).
98. Hamze-Komaiha, O., Sarr, S., Arlot-Bonnemains, Y., Samuel, D. & Gassama-Diagne, A. SHIP2 regulates lumen generation, cell division, and ciliogenesis through the control of basolateral to apical lumen localization of Aurora A and HEF1. *Cell Rep.* **17**, 2738–2752 (2016).
99. O'Farrell, F. et al. Class III phosphatidylinositol-3-OH kinase controls epithelial integrity through endosomal LKB1 regulation. *Nat. Cell Biol.* **19**, 1412–1423 (2017).
100. Gassama-Diagne, A. et al. Phosphatidylinositol-3,4,5-trisphosphate regulates the formation of the basolateral plasma membrane in epithelial cells. *Nat. Cell Biol.* **8**, 963–970 (2006).
101. Peng, J. et al. Phosphoinositide 3-kinase p110 δ promotes lumen formation through the enhancement of apico-basal polarity and basal membrane organization. *Nat. Commun.* **6**, 5937 (2015).
102. Takahashi, K. & Yamanaka, S. Induction of pluripotent stem cells from mouse embryonic and adult fibroblast cultures by defined factors. *Cell* **126**, 663–676 (2006).
103. Hoffding, M. K. & Hyttel, P. Ultrastructural visualization of the mesenchymal-to-epithelial transition during reprogramming of human fibroblasts to induced pluripotent stem cells. *Stem Cell Res.* **14**, 39–53 (2015).
104. Subramanyam, D. et al. Multiple targets of miR-302 and miR-372 promote reprogramming of human fibroblasts to induced pluripotent stem cells. *Nat. Biotechnol.* **29**, 443–448 (2011).
105. Li, R. et al. A mesenchymal-to-epithelial transition initiates and is required for the nuclear reprogramming of mouse fibroblasts. *Cell Stem Cell* **7**, 51–63 (2010).
106. Hansson, J. et al. Highly coordinated proteome dynamics during reprogramming of somatic cells to pluripotency. *Cell Rep.* **2**, 1579–1592 (2012).
107. Samavarchi-Tehrani, P. et al. Functional genomics reveals a BMP-driven mesenchymal-to-epithelial transition in the initiation of somatic cell reprogramming. *Cell Stem Cell* **7**, 64–77 (2010).
108. Choi, B. et al. Stiffness of hydrogels regulates cellular reprogramming efficiency through mesenchymal-to-epithelial transition and stemness markers. *Macromol. Biosci.* **16**, 199–206 (2016).
109. Downing, T. L. et al. Biophysical regulation of epigenetic state and cell reprogramming. *Nat. Mater.* **12**, 1154–1162 (2013).
110. Sakurai, K. et al. Kinome-wide functional analysis highlights the role of cytoskeletal remodeling in somatic cell reprogramming. *Cell Stem Cell* **14**, 523–534 (2014).
111. Di Stefano, B. et al. C/EBP α poises B cells for rapid reprogramming into induced pluripotent stem cells. *Nature* **506**, 235–239 (2014).
112. Gao, S. et al. Genome-wide gene expression analyses reveal unique cellular characteristics related to the amenability of HPC/HSCs into high-quality induced pluripotent stem cells. *Stem Cell Res Ther.* **7**, 40 (2016).
113. An, J., Zheng, Y. & Dann, C. T. Mesenchymal to epithelial transition mediated by CDH1 promotes spontaneous reprogramming of male germline stem cells to pluripotency. *Stem Cell Rep.* **8**, 446–459 (2017).
114. Hu, X. et al. Tet and TDG mediate DNA demethylation essential for mesenchymal-to-epithelial transition in somatic cell reprogramming. *Cell Stem Cell* **14**, 512–522 (2014).
115. Huang, P. et al. Induction of functional hepatocyte-like cells from mouse fibroblasts by defined factors. *Nature* **475**, 386–389 (2011).
116. Lim, K. T. et al. Small molecules facilitate single factor-mediated hepatic reprogramming. *Cell Rep.* **15**, 814–829 (2016).
117. Sekiya, S. & Suzuki, A. Direct conversion of mouse fibroblasts to hepatocyte-like cells by defined factors. *Nature* **475**, 390–393 (2011).
118. Cao, S. et al. Chemical reprogramming of mouse embryonic and adult fibroblast into endoderm lineage. *J. Biol. Chem.* **292**, 19122–19132 (2017).
119. D'Amour, K. A. et al. Efficient differentiation of human embryonic stem cells to definitive endoderm. *Nat. Biotechnol.* **23**, 1534–1541 (2005).
120. Li, Q. et al. A sequential EMT–MET mechanism drives the differentiation of human embryonic stem cells towards hepatocytes. *Nat. Commun.* **8**, 15166 (2017).
121. Liu, X. et al. Sequential introduction of reprogramming factors reveals a time-sensitive requirement for individual factors and a sequential EMT–MET mechanism for optimal reprogramming. *Nat. Cell Biol.* **15**, 829–838 (2013).
122. Maherali, N. & Hochedlinger, K. Tgfb β signal inhibition cooperates in the induction of iPSCs and replaces Sox2 and cMyc. *Curr. Biol.* **19**, 1718–1723 (2009).
123. Polo, J. M. et al. A molecular roadmap of reprogramming somatic cells into iPS cells. *Cell* **151**, 1617–1632 (2012).
124. Liang, G., He, J. & Zhang, Y. Kdm2b promotes induced pluripotent stem cell generation by facilitating gene activation early in reprogramming. *Nat. Cell Biol.* **14**, 457–466 (2012).
125. Onder, T. T. et al. Chromatin-modifying enzymes as modulators of reprogramming. *Nature* **483**, 598–602 (2012).
126. Wang, T. et al. The histone demethylases Jhdmla/1b enhance somatic cell reprogramming in a vitamin-C-dependent manner. *Cell Stem Cell* **9**, 575–587 (2011).
127. Mathieu, J. & Ruohola-Baker, H. Metabolic remodeling during the loss and acquisition of pluripotency. *Development* **144**, 541–551 (2017).
128. Shyh-Chang, N. et al. Influence of threonine metabolism on S-adenosylmethionine and histone methylation. *Science* **339**, 222–226 (2013).
129. Shiraki, N. et al. Methionine metabolism regulates maintenance and differentiation of human pluripotent stem cells. *Cell Metab.* **19**, 780–794 (2014).
130. Carey, B. W., Finley, L. W., Cross, J. R., Allis, C. D. & Thompson, C. B. Intracellular α -ketoglutarate maintains the pluripotency of embryonic stem cells. *Nature* **518**, 413–416 (2015).
131. Moussaieff, A. et al. Glycolysis-mediated changes in acetyl-CoA and histone acetylation control the early differentiation of embryonic stem cells. *Cell Metab.* **21**, 392–402 (2015).
132. Hay, E. D. The mesenchymal cell, its role in the embryo, and the remarkable signaling mechanisms that create it. *Dev. Dyn.* **233**, 706–720 (2005).
133. Han, X. et al. Mapping the mouse cell atlas by Microwell-seq. *Cell* **172**, 1091–1107 (2018).

134. Tan, T. Z. et al. Epithelial–mesenchymal transition spectrum quantification and its efficacy in deciphering survival and drug responses of cancer patients. *EMBO Mol. Med.* **6**, 1279–1293 (2014).
135. Grande, M. T. et al. Snail1-induced partial epithelial-to-mesenchymal transition drives renal fibrosis in mice and can be targeted to reverse established disease. *Nat. Med.* **21**, 989–997 (2015).
136. Lovisa, S. et al. Epithelial-to-mesenchymal transition induces cell cycle arrest and parenchymal damage in renal fibrosis. *Nat. Med.* **21**, 998–1009 (2015).
137. Cronan, M. R. et al. Macrophage epithelial reprogramming underlies mycobacterial granuloma formation and promotes infection. *Immunity* **45**, 861–876 (2016).
138. Thiery, J. P. Epithelial–mesenchymal transitions in tumour progression. *Nat. Rev. Cancer* **2**, 442–454 (2002).
139. Lambert, A. W., Pattabiraman, D. R. & Weinberg, R. A. Emerging biological principles of metastasis. *Cell* **168**, 670–691 (2017).
140. Mani, S. A. et al. The epithelial–mesenchymal transition generates cells with properties of stem cells. *Cell* **133**, 704–715 (2008).
141. Akalay, I. et al. Epithelial-to-mesenchymal transition and autophagy induction in breast carcinoma promote escape from T-cell-mediated lysis. *Cancer Res.* **73**, 2418–2427 (2013).
142. Noman, M. Z. et al. The immune checkpoint ligand PD-L1 is upregulated in EMT-activated human breast cancer cells by a mechanism involving ZEB-1 and miR-200. *Oncoimmunology* **6**, e1263412 (2017).
143. Terry, S. et al. Acquisition of tumor cell phenotypic diversity along the EMT spectrum under hypoxic pressure: consequences on susceptibility to cell-mediated cytotoxicity. *Oncoimmunology* **6**, e1271858 (2017).
144. Antony, J. et al. The GAS6–AXL signaling network is a mesenchymal (Mes) molecular subtype-specific therapeutic target for ovarian cancer. *Sci. Signal.* **9**, ra97 (2016).
145. Stockwell, B. R. et al. Ferroptosis: a regulated cell death nexus linking metabolism, redox biology, and disease. *Cell* **171**, 273–285 (2017).
146. Hangauer, M. J. et al. Drug-tolerant persister cancer cells are vulnerable to GPX4 inhibition. *Nature* **551**, 247–250 (2017).
147. Viswanathan, V. S. et al. Dependency of a therapy-resistant state of cancer cells on a lipid peroxidase pathway. *Nature* **547**, 453–457 (2017).
148. Datta, A., Bryant, D. M. & Mostov, K. E. Molecular regulation of lumen morphogenesis. *Curr. Biol.* **21**, R126–R136 (2011).
149. Peng, J. & Gassama-Diagne, A. Apicobasal polarity and Ras/Raf/MEK/ERK signalling in cancer. *Gut* **66**, 986–987 (2017).
150. He, S. et al. Sequential EMT–MET induces neuronal conversion through Sox2. *Cell Discov.* **3**, 17017 (2017).

Acknowledgements

We thank R. Jackson for her expert editing, K. Campbell, J. Casanova and E. Tzahor for advice and J. Peng for the artwork. D.P., X.S. and J.P.T. are supported by the National Natural Science Foundation of China (31421004) and the Key grant from the Guangdong Science and Technology Foundation of Guangdong Province (2017B030314056). A.G.-D. is supported by INSERM and the Ligue contre le Cancer.

Author contributions

All authors contributed equally to the Review.

Competing interests

The authors declare no competing interests.

Additional information

Reprints and permissions information is available at www.nature.com/reprints.

Correspondence should be addressed to D.P. or J.P.T.

Publisher's note: Springer Nature remains neutral with regard to jurisdictional claims in published maps and institutional affiliations.

© Springer Nature Limited 2019